Desalination and Water Treatment
www.deswater.com

doi: 10.5004/dwt.2022.28887

273 (2022) 34–42
October

The overall efficiency of a solar panel under various conditions

Badia Rtimi[a,*], Ali Benhmidene[a], Mehdi Dhaoui[b], Bechir Chaouachi[a]

[a]*Laboratory of Energy, Water, Environment and Processes, The National School of Engineering of Gabès, Gabès University, Tunisia, emails: rtimi.badiaa94@gmail.com (B. Rtimi), ali.benhmidene@gmail.com (A. Benhmidene), bechir.chaouachi@enig.rnu.tn (B. Chaouachi)*
[b]*Research Unit of Photovoltaic, Wind and Geothermal Systems, The National School of Engineering of Gabès, Gabès University, Tunisia, email: dhaouim@yahoo.fr*

Received 3 April 2022; Accepted 21 August 2022

ABSTRACT

The standard photovoltaic solar panels are characterized by their low efficiency, especially at high ambient temperatures. Cooling with water and nanofluid has been one of the most promising cooling strategies used to minimize the temperature of the PV module and improve the performance of the system. The main objective of this paper is to compare the performance of a PV panel located in the Gabes region in different cases: standalone PV panel, PV/T system with water-cooling, and PV/T system with nanofluid cooling. The tested fluids flow in a rectangular heat exchanger to maximize the contact area between the cooling fluid and the back wall of the solar panel. The influence of mass flow rate, nanofluid mass fraction, and nanofluid type on PV cell temperature, thermal, and electrical efficiency are investigated. The simulation results show that MgO is the best nanofluid in our working conditions and the electrical energy produced by MgO is 77.04 W/m^2. In addition, the thermal energy produced by MgO-water nanofluids is higher than that of other nanofluids. To highlight the benefits of using a rectangular heat exchanger mounted on the back of the panel, we compared its performance with that of a standalone photovoltaic panel. The results show that using a PV/T system with a flowing nanofluid inside improves the electrical power by 26.28 W/m^2 compared to a standalone PV panel.

Keywords: PV panel; Water; Nanofluid; Cooling; Efficiency

1. Introduction

Global water consumption is rising at over twice the rate of population growth due to higher living standards and increasing demand [1]. It is forecasted to increase by 50% in the next five years, due to the increase in the standard of living [2]. The use of reverse osmosis (RO) desalination units has increased significantly because of water shortages. Although constant efficiency improvements, RO desalination is still an energy-intensive process. Several studies have focused on the use of renewable energy sources such as solar photovoltaic (PV), to power small-scale RO plants.

Solar panels work properly only under certain weather conditions, however, the climate is usually changing and solar panels are installed in different climates around the world that's why most panels do not work well under various conditions [3].

To overcome this problem, engineers need to understand how solar panels react to these different conditions. In fact, the electrical efficiency of the PV module is affected by its surface rise in temperature [4]. For instance, the efficiency of crystalline silicon solar cells falls by 0.5% for every 1°C rise in solar cell temperature and this decrease in efficiency varies with the type of cell [5]. The increase in PV cell temperature and heat loss are reduced using a non-inflammable fluid, which flows under the PV panel and behaves as a heat exchanger, therefore, enhancing the thermal efficiency of the system. Such sort of system

* Corresponding author.

1944-3994/1944-3986 © 2022 Desalination Publications. All rights reserved.

can provide thermal and electrical energy at the same time, which is called photovoltaic thermal (PVT) system. One of the advantages of the PVT system is the combined generation of thermal and electrical energy, which makes it more efficient than standalone PV collectors [6]. Several studies have used this type of technology and compared its performance with that of the standalone PV panel. For instance, Yu et al. [7] used the PVT panel and showed experimentally that the system can gain 3.5% of electrical performance and 324.3% of overall output energy compared to a standalone PV system. In the same environment, Singh et al. [8] studied the effect of using oscillatory water flow on the PV cells' performance, the results show that a gain of an electrical efficiency from 0.2772% to 1.122% compared to a standalone PV module is recorded.

Another problem appears here, the traditional fluids such as water and oil, whose thermal conductivity and heat carrying capacity are very low, are not very effective in solar photovoltaic thermal (PVT) systems [9]. Thus, researchers and scientists are focusing to utilize a new kind of fluid that enhances thermal conductivity and heat capacity. One of the proposed solutions is the use of nanofluids. In fact, nanofluids are the best option to use in a solar photovoltaic thermal system [10] due to their properties [11]. These small particles mixed with a base fluid can absorb all the superfluous solar radiation, which is not usable for photovoltaic cells and hence decreasing the cell temperature. As a result, nanofluids could operate as an optical filter for PV cells [12].

Various studies have both experimentally and numerically researched the effects of nanofluids on the electrical and thermal efficiency of PVT collectors [13]. For example, Michael et al. [14] used CuO-water nanofluid as the HTF in a PVT collector; it was shown that the overall enhancement in yield of the PVT was improved by 19.25% compared to water. Al-Waeli et al. [15] investigated the PVT systems (conventional PV, water-based PVT, water-nanofluid PVT, and nanofluid/nano-PCM) under the same conditions and environment. The results show that using nanofluid/nano-PCM increases the electrical efficiency from 8.07% to 13.32%, and the thermal efficiency reaches 72%. In addition, Tong et al. [16], applied Al_2O_3/water nanofluid in a flat-plate solar collector and compared its efficiency with the case of using pure water. They observed that using the mentioned nanofluid could improve the efficiency up to 21.9%. Besides, Razali et al. [17] have presented recent advances in PVT systems using nanofluid. The results show that an effective heat transfer can increase the efficiency of the PVT system and power generation. As well, Okonkwo et al. [18] have shown that the presence of a nanosized colloidal dispersion in the fluid induces a better thermal conductivity. This increase in thermal conductivity is directly proportional to the volume concentration of the nanoparticles. Moreover, Rostami et al. [19] used the atomized CuO-nanofluid, the PV temperature decreased to 57.25% and the maximum power was 51.1% using a concentration of nanofluid between 0.01 and 0.8%, and a flow rate from 0.4 to 12.5 m^3/h.

There have also been several studies investigating the effect of mass flow rate on PVT systems. In this vein, Hossein Zadeh et al. [20] examined the effect of mass flow rate, absorbed solar irradiance, wind speed, and ambient temperature on the electrical and thermal efficiency of the PVT collector. The results indicated that at an optimum mass fraction of 12 wt.%, the thermal and electrical efficiency increase was 12.78% and 0.28% respectively. The study also highlighted that a rise in mass flow rate from 30 to 70 kg/h caused a significant increase in both the thermal and electrical efficiencies of the PVT. Furthermore, Tian et al. [21] simulated a simple solar panel with a cooling system for the operating conditions in China. The PVT working fluid is MgO/water. The results of this study show that enhancing the nanofluid flow in the cooling system makes the panel cooler and reduces the amount of exergy output. The addition of nanoparticles, especially at low nanofluid flow rates, enhances the exergy output. The results demonstrate that an increment in the flow rate from 0.5 to 4 l/min reduces the efficiency by 2.03%. Adding 1% of nanoparticles increases the exergy efficiency by 0.45% at a volume flow rate of 0.5 l/min.

Various researches have studied the effect of nanofluid type and concentration on the performance of PV panels. Jia et al. [22] investigated the influence of nanofluid type and volume concentration on PV conversion efficiency, PV cell temperature, thermal and electrical power. In this study, Al_2O_3/water, TiO_2/water, and the base fluid are used as a working fluid. The results show that the performance of the PV/T collector with Al_2O_3/water is better than the PVT collector using TiO_2/water. When the mass flow rate of the nanofluid is 0.03 kg/s, the electrical power of the PVT collector is higher than that of the PVT collector when the mass flow rate of the nanofluid is 0.0005, 0.001, and 0.01 kg/s. They found that when the volume concentration increases, the efficiency of the panel increases in turn and these values are 0.28% when the volume concentration is 3% compared to water, 0.07% when the volume concentration is 3%–6%.

The main objective of this paper is to improve the efficiency of PVT panels using various nanofluids nature inside the cooling system. These fluids were circulated through a rectangular heat exchanger mounted at the back of the panel. The effects of the mass fraction of nanoparticles ($1\% \le \phi \le 9\%$) and the flow rate of nanofluid (0.001–0.02 s kg/s) are numerically studied using the Matlab software. A comparison between standalone PV panel, PVT panel with water-cooling, and PVT panel with nanofluid cooling was established in order to determine the amount of gained power

2. Modeling the photovoltaic panel

The PVT system contains glass, solar cell (PV), tedlar layer, heat exchanger, and an insulating layer. The proposed system is represented in Fig. 1. The received solar energy is absorbed by the glass and then transferred to the photovoltaic cell. Over time the PV cell temperature rises and heat is transferred to the tedlar layer, then to the fluid inside the heat exchanger, and finally, a small amount of energy is transferred to the insulating layer. The purpose of the energy balance is to take advantage of the cooling process for thermal storage and electrical efficiency improvement. In the energy balance, the following assumptions were made:

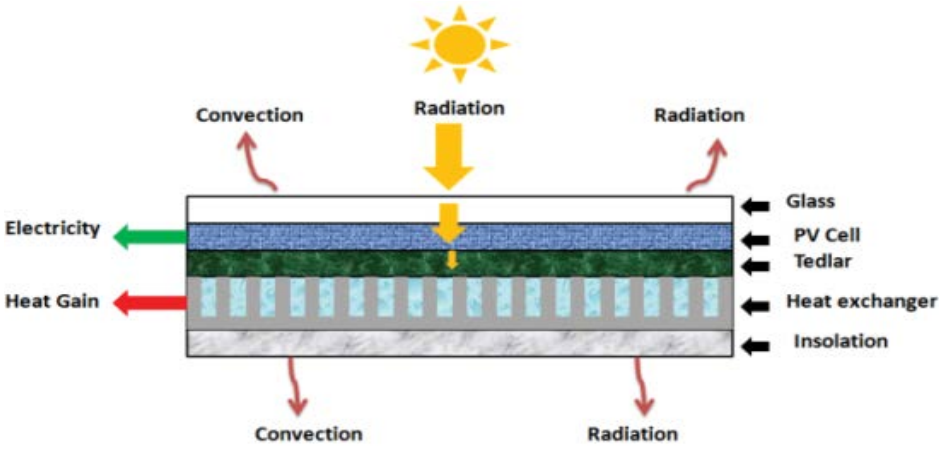

Fig. 1. The PV panel components.

- All surfaces of the PVT system had the same area.
- There is no dust or partial shading on the collector.
- The temperature variation along the system is linear.
- The adopted meteorological data of the region of Gabes are latitude = 33°53′17.077″N, longitude = 10°5′51.079″E.
- The flow is fully developed in the tubes.
- The effect of the friction in the pipes is neglected.

The energy balance is a set of equations that represents the amount of accumulated energy that is equal to the difference between the input and output energy.

2.1. Energy balance on the glass

Glass temperature T_g is defined from the energy balance of the glass where it's given as follows [23]:

$$\frac{dT_g}{dt}=\frac{1}{m_g c_g}\begin{pmatrix}\alpha_g I_g A_g-\left(5.7+3.8U_V\right)A_g\left(T_g-T_a\right)\\-\sigma\varepsilon_g A_g\left(T_g^4-T_{\text{sky}}^4\right)-\dfrac{k_g}{\delta_g}A_g\left(T_g-T_c\right)\end{pmatrix} \tag{1}$$

The sky temperature is related to the ambient temperature by the following relationship [23]:

$$T_{\text{sky}}=0.0552\times T_a^{1.5} \tag{2}$$

where I_G: solar radiation (w/m²); U_V: wind velocity (m/s); T_g, T_a: glass and ambient temperature; σ: Boltzmann constant; K_g, δ_g, α_g, ε_g, A_g: thermal conductivity, thickness, absorption factor, emissivity and surface of glass.

2.2. Energy balance on PV cells

The variation of cell temperature against time is given by the following differential equation [23]:

$$\frac{dT_c}{dt}=\frac{1}{m_c c_c}\begin{pmatrix}\tau_g A_g\alpha_c\beta_c I_G+\dfrac{K_g}{\delta_g}A_g\left(T_g-T_c\right)\\-\left(\dfrac{k_c}{\delta_c}+\dfrac{k_t}{\delta_t}\right)A_c\left(T_c-T_t\right)-E_c A_c\end{pmatrix} \tag{3}$$

where α_c, β_c, k_c, A_c, δ_c: absorption coefficient, fill factor, thermal conductivity, surface, thickness of cell; δ_t, k_t: thickness, thermal conductivity of the tedlar layer; T_c, T_t: cell temperature and tedlar temperature.

The electrical energy generated by a solar panel is a function of cell temperature T_c, referred cell temperature $T_{c,\text{ref}}$, as follows [24]:

$$E_c=\alpha_c\tau_g\beta_c I_G A_g\eta_{\text{ref}}\left(1-\theta\left(T_c-T_c-T_{c,\text{ref}}\right)\right) \tag{4}$$

where η_{ref}, $T_{c,\text{ref}}$: reference yields and temperature.

2.3. Energy balance on the Tedlar

The variation of cell temperature against time is given by the following differential equation [23]:

$$\frac{dT_t}{dt}=\frac{1}{m_t c_t}\begin{pmatrix}\left(\dfrac{k_c}{\delta_c}+\dfrac{k_t}{\delta_t}\right)A_c\left(T_c-T_t\right)-\dfrac{N_u k_f}{D_h}A_t\left(T_t-T_f\right)\\-\dfrac{\sigma\left(T_t+T_{\text{co}}\right)\left(T_t^2+T_{\text{co}}^2\right)}{\dfrac{1}{\varepsilon_{\text{co}}}+\dfrac{1}{\varepsilon_t}-1}A_t\left(T_t-T_{\text{co}}\right)\\+A_t\tau_g\left(1-\beta_c\right)\alpha_t I_G\end{pmatrix} \tag{5}$$

where Nu: Nusselt number; k_f, T_f: thermal conductivity and temperature of fluid; D_h: hydraulic diameter; α_t, T_t: absorption coefficient and temperature of tedlar layer; ε_{co}: emissivity of the pipe.

2.4. Energy balance on the cooling fluid

The temperature of fluid along the panel is deduced by the energy balance given by the Eq. (6).

$$\frac{dT_f}{dt}=\frac{1}{m_f c_f}\begin{pmatrix}\left(C_f\dot{m}_f T_{i,f}-C_f\dot{m}_f T_{o,f}\right)A_f\\+\dfrac{N_u k_f}{D_h}\begin{pmatrix}A_t\left(T_t-T_f\right)-A_f\left(T_f-T_{\text{co}}\right)\\-S\left(T_f-T_{\text{amb}}\right)\end{pmatrix}\end{pmatrix} \tag{6}$$

where $T_{i,f}$ and $T_{o,f}$ are respectively the inlet and the outlet fluid temperature.

2.5. Thermal balance on the pipe

The cooling fluid flows along the rectangular pipe. The balancing energy for the wall pipe is:

$$\frac{dT_{co}}{dt}=\frac{1}{m_{co}c_{co}}\left(\begin{array}{l}\dfrac{\sigma\left(T_t+T_{co}\right)\left(T_t^2+T_{co}^2\right)}{\dfrac{1}{\varepsilon_{co}}+\dfrac{1}{\varepsilon_t}-1}A_t\left(T_t-T_{co}\right)\\ +A_f\dfrac{N_uK_f}{D_H}\left(T_f-T_{co}\right)-\dfrac{k_{co}}{e_{co}}A_{co}\left(T_{co}-T_a\right)\\ -\sigma\varepsilon_{co}\left(T_{sol}-T_{co}\right)\left(T_{sol}^2+T_{co}^2\right)A_{co}\left(T_{co}-T_{sol}\right)\end{array}\right) \quad (7)$$

3. Simulation's results

The purpose of the present numerical study is the selection of suitable nanoparticles for the heat exchanger. To achieve this goal, the considered nonmaterial are Al_2O_3, Cu, SWCNT, MgO, SiO_2. The numerical simulation is run using Matlab software. The following considerations were taken into account:

- The calculations are performed from an initial time "t_0" for each component, at an initial temperature equal to the ambient temperature.
- The meteorological data of the region of Gabes located in southern Tunisia are latitude = 33° 53′ 17.077″N, longitude = 10° 5′ 51.079″E.

The choice of the most suitable nanofluid is based on its effect on the characteristic of the PVT panel, namely:

- The temperature of the cell
- Electric and thermal efficiency of the panel
- Electric and thermal power

3.1. Model validation

The theoretical model is validated by comparing the electrical performance results obtained from the simulation with the electrical performance results obtained from the experiments of Alzaabi et al. [25]. In the case of water-cooled photovoltaic modules. The selection of these results is due to the fact that the authors used the same geometric heat exchanger in addition to the internal coolant. The heat exchanger in the Alzaabi et al. experiment consists of 11 rectangular copper tubes attached to the back of a polycrystalline PV module. Tube dimensions are 0.5 inch and 0.25 inch. The panel area is 1.17 × 0.67 m^2. The coolant used in the experiment is water with a flow rate of 5.4 l/min.

Fig. 2 shows a comparison between the power obtained from the simulation and the power obtained from Alzaabi et al.'s experiments [25]. The power varies throughout the day, peaking between 12:00 and 14:00. The maximum power obtained by the model is about 75 W, while the experiments by Alzaabi et al. [25], about 81 W. The MAE and RMSD values are below 6.7%. This result shows a high degree of similarity between our simulation results and those of Alzaabi et al. [25].

3.2. Effect of mass flow rate

In order to improve higher electrical efficiency, the PV panel should be cooled with a heat exchange mechanism using fluid streams like nanofluid.

This cooling medium can improve the electrical efficiency, and decrease the rate of cell degradation with time, resulting in the maximization of the life span of photovoltaic modules.

Fig. 3 shows the variation of cell temperature for different values of flow rate. By increasing the flow rate, the cell temperature decreases gradually. In fact, for a flow rate equal to 0.001 kg/s this temperature goes from 53°C for SWCNT to 46.7°C for MgO. By increasing the flow rate to 0.01 kg/s the highest temperature value 42.39°C is recorded for SWCNT whereas the lowest value 41.63°C is registered for MgO.

For a flow rate equal to 0.02 kg/s, the cell temperature's lowest value is 40.51°C when using MgO. This reduction in cell temperature is due to the fact that the Reynolds number increases when the mass flow rate increases, which ultimately increases the heat transfer coefficient of the

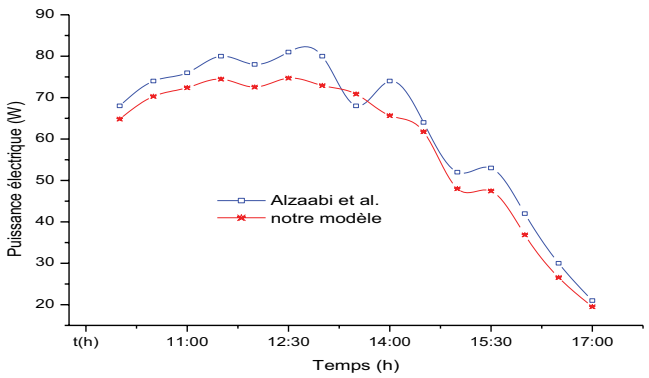

Fig. 2. Comparison of simulation results with those of Alzaabi et al. [25].

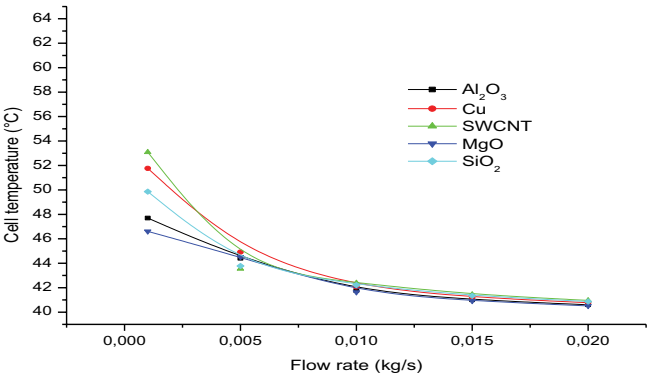

Fig. 3. Effect of flow rate on cell temperature.

tubes. As a result, more heat is removed from the cell at higher flow rates within the considered range.

By increasing the flow of nanofluid, the cell temperature decreases and consequently the electrical efficiency increases. For a flow rate equal to 0.001 kg/s the minimum efficiency value recorded is 12.42% for SWCNT and the maximum value is equal to 12.86% in the case of MgO. By increasing the water flow rate, the efficiency increases gradually for all the nanofluid types and the gap between them becomes very low especially for the entire value superior to 0.01 kg/s. In fact, for a flow rate equal to 0.02 kg/s the minimum-recorded efficiency value is 13.92% for SWCNT and the maximum value is equal to 13.95% in the case of MgO and Al_2O_3.

The thermal efficiency presents a different behavior vs. the nanofluid flow. Indeed, Fig. 5 shows that for flow rates ranging from 0.001 to 0.005 kg/s the thermal efficiency increases slowly. For flow rates ranging from 0.005 to 0.02 kg/s, the yields are increasing. The maximum yield value recorded is 80.13% for MgO and at a flow rate equal to 0.02 kg/s.

To summarize, the base fluid flow has a significant influence on the cell temperature, electrical and thermal efficiency. According to Figs. 4 and 5, if the flow rate exceeds 0.01 kg/s, the performance difference between all nanofluids becomes small. Therefore, the optimal flow to choose is 0.01 kg/s.

3.3. Effect of nanofluid mass fraction

Fig. 6 shows the variation of cell temperature for different nanofluid fractions ranging from 1% to 9% for a flow rate equal to 0.01 kg/s. The maximum temperature values are recorded for SWCNT, which goes from 44.43°C (ϕ = 1%) to 40.23°C (ϕ = 9%). The best performing nanofluid is MgO which guarantees a minimum cell temperature, the temperature goes from 43.53°C (ϕ = 1%) to 39.88°C (ϕ = 9%).

By increasing the fraction of nanofluid, the electrical efficiency increases progressively. Considering Fig. 7, the first and second performing nanofluids are respectively MgO and Al_2O_3. For ϕ = 1%, the maximum efficiency recorded is 13.75% for MgO and the minimum efficiency found is 13.69% for SWCNT. For ϕ = 9%, the maximum yield recorded is 13.99% for MgO and the minimum yield found is 13.95% for SiO_2.

Fig. 8 illustrates the variation of thermal efficiency for different values of nanoparticles fraction. By examining Fig. 8, we extract the following observations: The thermal

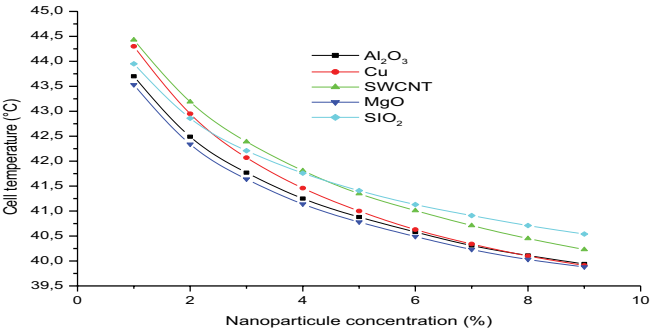

Fig. 6. Effect of nanofluid mass fraction on cell temperature.

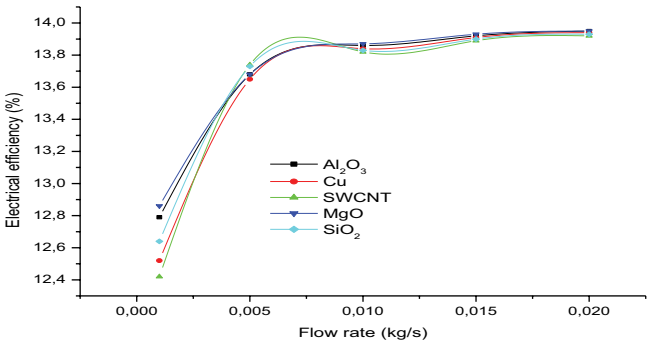

Fig. 4. Effect of flow rate on electrical efficiency.

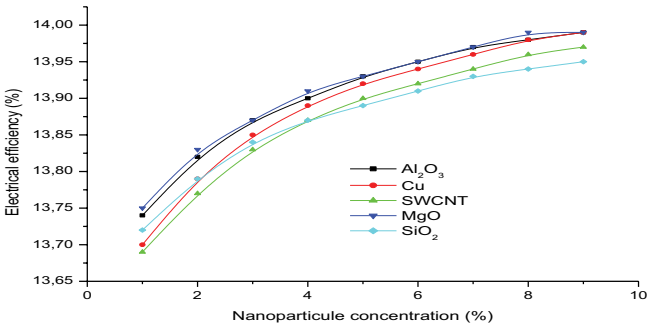

Fig. 7. Effect of nanofluid mass fraction on electrical efficiency.

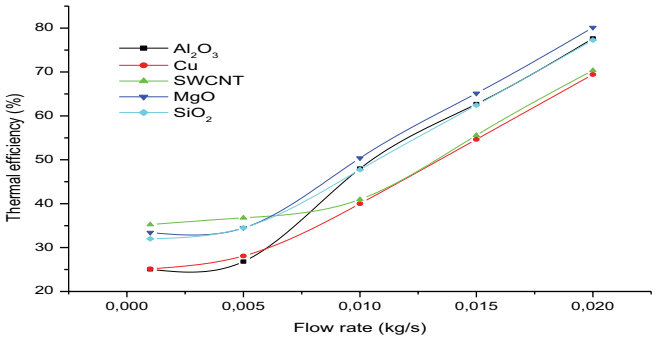

Fig. 5. Effect of flow rate on thermal efficiency.

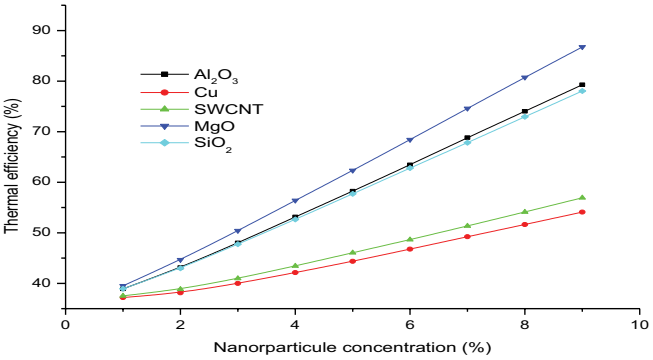

Fig. 8. Effect of nanofluid mass fraction on thermal efficiency.

efficiency increases with particle mass fraction. The worst nanofluid is the Cu, which ensures a minimal efficiency: for ϕ = 1% the efficiency is equal to 37.20% and for ϕ = 9% the efficiency is equal to 54.1%. The best performing nanofluid is MgO, the recorded yield values are 39.51% (ϕ = 1%) and 86.76% (ϕ = 9%).

The mass fraction of nanofluid is a very important parameter to study; indeed, by looking at the Fig. 8 we notice that the behavior of each nanofluid is different from one mass fraction interval to another. In each interval, the performances of nanofluids are different. For the cell temperature, the electrical efficiency, the performances of all the nanofluids in any mass fraction value are close, but for the thermal efficiency, the gap increases. The increase of nanofluid mass fraction improves the heat transfer coefficient of the fluid used and then the performance of our system. However, with high-value of mass fraction, many parameters increase such as the cost of implementation, the instability of the fluid (due to agglomeration), the friction factor, and the energy required for the pumping of the nanofluid and the global corrosion of the system. Taking into consideration all these factors, the optimal fraction chosen is 3% for the rest of the article.

3.4. Choice of nanofluid

In the following part, the value of flow and mass fraction of nanofluid are fixed. The aim of this part is to determine and verify the most efficient nanofluid for a solar installation in Gabes.

The results in Fig. 9 show that each nanoparticle acts differently on the cell temperature. The maximum temperature recorded is 42.39°C for SWCNT (Single-Walled Carbon Nanotubes). It is found that magnesium oxide (MgO) and Alumina (Al_2O_3) is the first-best and second-best alternatives, respectively. The temperature values recorded for MgO and Al_2O_3 are equal to 41.64°C and 41.77°C. Another advantage of using MgO nanoparticles is storing the maximum of thermal energy. In fact, the temperature of the outlet fluid in the panel is higher than the other nanoparticles used. The outlet temperature of nanofluid with MgO is 30.57°C. By considering an inlet temperature of 25°C, the increase of MgO-nanofluid is about 5°C.

The electrical efficiency for the studied solar panel decreases gradually with temperature. Fig. 10 presents the efficiency profile throughout the day for different nanofluids. When the radiation is maximum at 13:30 h, the efficiency for Al_2O_3, Cu, SWCNT, MgO, and SiO_2 is respectively 13.87%, 13.85%, 13.83%, 13.87%, and 13.84%.

The following diagram presents the maximum-recorded values of electrical energy for different nanofluids. The values found by the simulation are relatively close. The minimum-recorded value is 76.79 W/m² for SWCNT. The maximum-recorded value is 77.04 W/m² for MgO.

The second diagram presents the values recorded for maximum sunlight of the thermal energy. These values differ from one nanofluid to another and describe the capacity of a nanofluid to retain heat. The maximum value of thermal energy is 374.64 W/m² for MgO. The minimum value of thermal energy is 297.1 W/m² for Cu.

According to the Figs. 11 and 12, there is the MgO-nanofluid that ensures the highest electrical efficiency and guarantees the best thermal efficiency, that's why the best performing nanofluid is MgO.

3.5. Comparative study

To show the impact of the use of MgO-nonfluid on the performance of PV panels, a comparative study is the object of this section. Indeed, the cell temperature, as well as the electrical performance and the electrical power, are simulated for three cases of the panel; the first one is in absence of cooling, the second one is the flow of water with a mass flow rate of 0.01 kg/s and the third one is the used of MgO-nanofluid of 3% mass fraction and a flow rate of 0.01 kg/s.

The simulation results for the cell temperature and electric efficiency are shown in Figs. 13 and 14 respectively.

According to Fig. 13, the addition of a cooling system allows us to reduce the cell temperature from 111.86°C to 49.13°C so a reduction of 62.73°C has been approved. This significant reduction in temperature improves the electric efficiency (Fig. 14). Indeed, in maximum sunshine, the electric efficiency decreases to 9.14% in the case of PV, but in the PVT system, this value increases to 13.37%. In terms of electric power, the PV system produces 50.76 W/m²

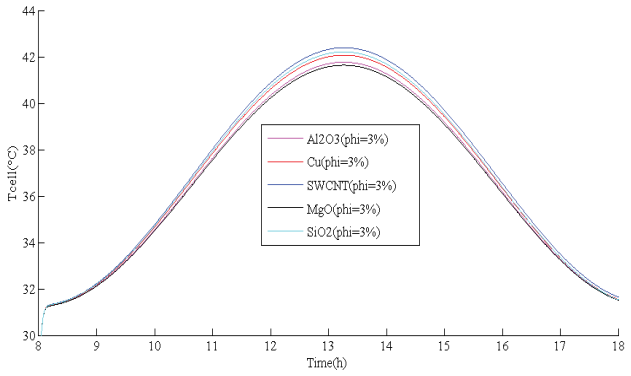

Fig. 9. Effect of variation of nanofluid nature on the cell temperature.

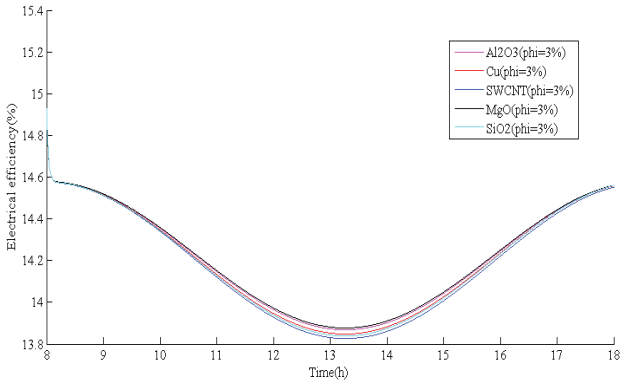

Fig. 10. Effect of variation of nanofluid nature on the electrical efficiency.

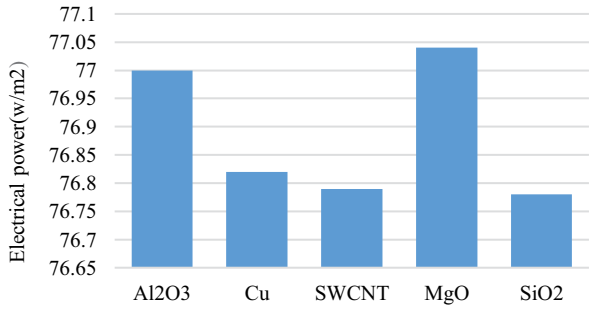

Fig. 11. Effect of nanofluid nature on the electrical power generation.

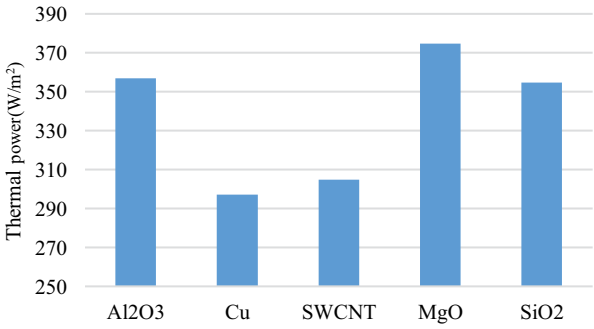

Fig. 12. Effect of nanofluid nature on the thermal power.

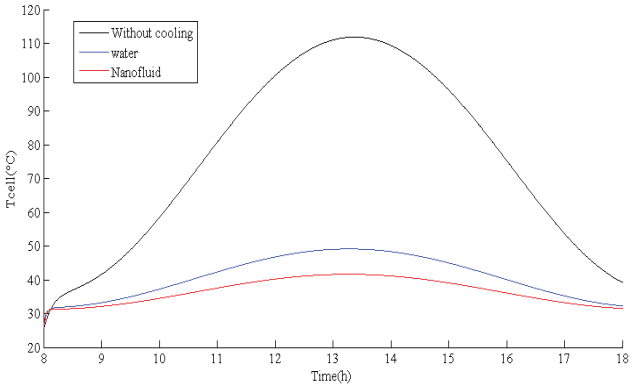

Fig. 13. Cell temperature in different cases.

while the PVT system produces 77.04 W/m², so a gain of 26.28 W/m² is recorded.

4. Conclusion

In the present paper, the thermal behavior of a hybrid PVT panel with a rectangular heat exchanger is modeled. The energy equations for the different components of PVT panel are resolved using the Runge-Kutta method in Matlab software. The simulation results focused on the effect of some parameters such as nanofluid flow rate, nanoparticle mass fraction, and nanoparticle type on the performance of a solar panel. As a result, the electrical energy produced using various types of nanofluids is between 76.79 and 77.04 W/m². When it comes to the thermal energy

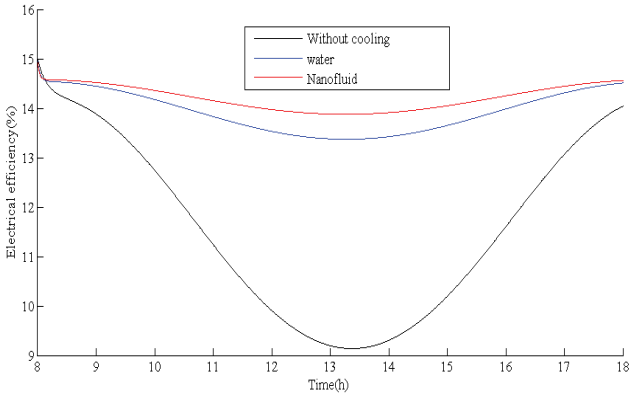

Fig. 14. Electrical efficiency profile in different cases.

produced, MgO-water and Al_2O_3-water are the first and second nanofluids. Indeed, the thermal energy was respectively 374.64 and 356.84 W/m². According to the overall energy, MgO-water is the best nanofluid for the current cooling system. The use of such a system with MgO-Water nanofluid at a mass flow rate of 0.01 kg/s and a mass fraction of 3% inside the rectangular heat exchanger improves the electrical power by 26.28 W/m² compared to a standalone PV panel.

Symbols

U_v	—	Wind velocity, m/s
T	—	Average temperature, °C
A	—	Surface area, m²
m	—	Mass, kg
c	—	Heat capacity, kJ/kg·K
k	—	Thermal conductivity, W/m·K
E	—	Energy produced, W
D	—	Hydraulic diameter of the channel, m
$\dot{m}$	—	Mass flow rate of fluid, kg/s
Pr	—	Prandtl number
Re	—	Reynolds number
S	—	Heat exchange surface with the outside environment, m²

Greek

A	—	Absorption factor
η	—	Electrical efficiency
τ	—	Transmissivity
B	—	Fill factor
ρ	—	Density
θ	—	Coefficient de temperature du silicium
Φ	—	Mass fraction of the MgO nanoparticles

Subscripts

G	—	Glass
C	—	Cell
T	—	Tedlar
Nf	—	Nanofluid
Np	—	Nanoparticle

Bf	—	Base fluid
H	—	Hydraulic
F	—	Fluid
Ct	—	Between cell and tedlar
s,f	—	Outlet fluid
e,f	—	Inlet fluid
amb	—	Ambiant

References

[1] M.M. Mekonnen, A.Y. Hoekstra, Four billion people facing severe water scarcity, Sci. Adv., 2 (2016) 6, doi: 10.1126/sciadv.1500323.

[2] UN-Habitat, World Cities Report, 2016.

[3] R. Sheps, P. Golovinsky, S. Yaremenko, T. Shchukina, New passive solar panels for Russian cold winter conditions, Energy Build., 248 (2021) 111187, doi: 10.1016/j.enbuild.2021.111187.

[4] L. Idoko, O. Anaya-Lara, A. McDonald, Enhancing PV modules efficiency and power output using multi-concept cooling technique, Energy Rep., 4 (2018) 357–369.

[5] A. Razak, M.I. Yusoff, L.W. Zhe, M. Irwanto, S. Ibrahim, M. Zhafarina, Investigation of the effect temperature on photovoltaic (PV) panel output performance, Int. J. Adv. Sci. Eng. Inf. Technol., 6 (2016) 682–688.

[6] L.K. Alexis, T.J. Kewir, D.K.B. Merlain, S.S.H. Bertholt, Experimental study on the electrical and thermal characteristics of a hybrid photovoltaic/thermal water solar collector model using photovoltaic solar modules of different brands, Energy Convers. Manage.: X, 14 (2022) 100198, doi: 10.1016/j.ecmx.2022.100198.

[7] M. Yu, F. Chen, S. Zheng, J. Zhou, X. Zhao, Z. Wang, G. Li, J. Li, Y. Fan, J. Ji, T.M.O. Diallo, D. Hardy, Experimental investigation of a novel solar micro-channel loop-heat-pipe photovoltaic/thermal (MC-LHP-PV/T) system for heat and power generation, Appl. Energy, 256 (2019a) 113929, doi: 10.1016/j.apenergy.2019.113929.

[8] S. Singh, R. Singh, G. Tiwari, Effect of Oscillatory Water Flow on the Performance of Photovoltaic Thermal System in Summer Condition, International Conference on Computational and Characterization Techniques in Engineering & Sciences (CCTES) Integral University, Lucknow, India, Sep 14–15, 2018, doi: 10.1109/CCTES.2018.8674075.

[9] S.R. Reddy, M.A. Ebadian, C.-X. Lin, A review of PV–T systems: thermal management and efficiency with single-phase cooling, Int. J. Heat Mass Transfer, 91 (2015) 861–871.

[10] A.K. Suresh, S. Khurana, G. Nandan, G. Dwivedi, S. Kumar, Role on nanofluids in cooling solar photovoltaic cell to enhance overall efficiency, Mater. Today: Proc., 5 (2018) 20614–20620.

[11] A.S. Abdelrazik, F.A. Al-Sulaiman, R. Saidur, Optical behavior of a water/silver nanofluid and their influence on the performance of a photovoltaic-thermal collector, Sol. Energy Mater. Sol. Cells, 201 (2019) 110054, doi: 10.1016/j.solmat.2019.110054.

[12] A.S. Abdelrazik, F.A. Al-Sulaiman, R. Saidur, R. Ben-Mansour, A review on recent development for the design and packaging of hybrid photovoltaic/thermal (PV/T) solar systems, Renewable Sustainable Energy Rev., 95 (2018) 110–129.

[13] C. Kalkan, M.A. Ezan, J. Duquette, S. Yilmaz Balaman, A. Yilanci, Numerical study on photovoltaic/thermal systems with extended surfaces, Int. J. Energy Res., 43 (2019) 5213–5229.

[14] J.J. Michael, S. Iniyan, Performance analysis of a copper sheet laminated photovoltaic thermal collector using copper oxide – water nanofluid, Sol. Energy, 119 (2015) 439–451.

[15] A.H.A. Al-Waeli, K. Sopian, J.H. Yousif, H.A. Kazem, J. Boland, M.T. Chaichan, Artificial neural network modeling and analysis of photovoltaic/thermal system based on the experimental study, Energy Convers. Manage., 186 (2019a) 368–379.

[16] Y. Tong, H. Lee, W. Kang, H. Cho, Energy and exergy comparison of a flat-plate solar collector using water, Al_2O_3 nanofluid, and CuO nanofluid, Appl. Therm. Eng., 159 (2019) 113959, doi: 10.1016/j.applthermaleng.2019.113959.

[17] N.F.M. Razali, A. Fudholi, M.H. Ruslan, K. Sopian, Review of water-nanofluid based photovoltaic/thermal (PV/T) systems, Int. J. Electr. Comput. Eng., 9 (2019) 134–140.

[18] E.C. Okonkwo, I. Wole-Osho, D. Kavaz, M. Abid, Comparison of experimental and theoretical methods of obtaining the thermal properties of alumina/iron mono and hybrid nanofluids, J. Mol. Liq., 292 (2019) 111377, doi: 10.1016/j.molliq.2019.111377.

[19] Z. Rostami, M. Rahimi, N. Azimi, Using high-frequency ultrasound waves and nano-fluid for increasing the efficiency and cooling performance of a PV module, Energy Convers. Manage., 160 (2018) 141–149.

[20] M. Hosseinzadeh, M. Sardarabadi, M. Passandideh-Fard, Energy and exergy analysis of nanofluid based photovoltaic thermal system integrated with phase change material, Energy, 147 (2018) 636–647.

[21] M.-W. Tian, Y. Khetib, S.-R. Yan, M. Rawa, M. Sharifpur, G. Cheraghian, A.A. Melaibari, Energy, exergy and economics study of a solar/thermal panel cooled by nanofluid, Case Stud. Therm. Eng., 28 (2021) 101481, doi: 10.1016/j.csite.2021.101481.

[22] Y. Jia, F. Ran, C. Zhu, G. Fang, Numerical analysis of photovoltaic-thermal collector using nanofluid as a coolant, Sol. Energy, 196 (2020) 625–636.

[23] Z.U. Abdin, A. Rachid, Modeling, Identification and Control of Photovoltaic/Thermal Solar Panel, 2020 IEEE Conference on Control Technology and Applications (CCTA), IEEE, Montreal, QC, Canada, 2020, pp. 1–6, doi: 10.1109/CCTA41146.2020.9206348.

[24] T. Brahim, A. Jemni, Parametric study of photovoltaic/thermal wickless heat pipe solar collector, Energy Convers. Manage., 239 (2021) 114236, doi: 10.1016/j.enconman.2021.114236.

[25] A.A. Alzaabi, N.K. Badawiyeh, H.O. Hantoush, A.-K. Hamid, Electrical/thermal performance of hybrid PV/T system in Sharjah, UAE, Int. J. Smart Grid Clean Technol., 3 (2014) 385–389.

[26] S. El Bécaye Maïga, S.J. Palm, C.T. Nguyen, G. Roy, N. Galanis, Heat transfer enhancement by using nanofluids in forced convection flows, Int. J. Heat Fluid Flow, 26 (2005) 530–546.

[27] S. El Bécaye Maïga, C.T. Nguyen, N. Galanis, G. Roy, Heat behaviors of nanofluids in a uniformly heated tube, Superlattices Microstruct., 35 (2004) 543–557.

[28] G.K. Batchelor, The effect of Brownian motion on the bulk stress in a suspension of spherical particles, J. Fluid Mech., 831 (1977) 97–117.

[29] J. Maxwell, A Treatise on Electricity and Magnetism, Oxford University Press, Cambridge, UK, 1904.

[30] B.C. Pak, Y.I. Cho, Hydrodynamic and heat transfer study of dispersed fluids with submicron metallic oxide particles, Exp. Heat Transfer, 11 (1998) 151–170.

Appendix

The physical properties of nanofluids depend on parameters including the thermal properties of water as the base fluid and the volume fraction of nanoparticles dispersed in water. Based on the report of Maiga et al., [26], the equations below are general relationships used to calculate the specific heat and density for a conventional two-phase mixture.

The specific heat of nanofluid can be calculated by [27]:

$$cp_{nf} = (1-\varphi)cp_{water} + \varphi cp_{np} \tag{8}$$

The density of the nanofluid is calculated by the following relation [28]:

$$\rho_{nf} = (1-\varphi)\rho_{water} + \varphi\rho_{np} \tag{9}$$

Batchelor studied theoretically the dynamic viscosity of a nanofluid taking into account the effect of the hydrodynamic interaction between two spherical nanoparticles. He showed that the dynamic viscosity of a nanofluid is not a linear function of the volume fraction as the relations of [29]:

$$\mu_{nf} = \left(1 + 2.5\varphi + 6.2\varphi^2\right)\mu_{water} \tag{10}$$

Regarding the thermal conductivity of the nanofluid, is approximated by the Maxwell–Garnetts model [30]:

$$k_{nf} = k_{water} \times \left(\frac{k_{np} + 2\times k_{bf} + 2\times\varphi\left(k_{np} - k_{bf}\right)}{k_{np} + 2\times k_{bf} - 2\times\varphi\left(k_{np} - k_{bf}\right)} \right) \tag{11}$$

The physical properties of different nanoparticles are presented in Table 1.

The root mean square of the relative error RMSD is defined as:

$$\mathrm{RMSD}(\%) = 100 \times \sqrt{\frac{\sum_1^N \frac{{}^{th}X(i)^{-x}\exp(i)^2}{{}^{th}X(i)}}{N}} \tag{12}$$

The Mean absolute percent error MAE is calculated by:

$$\mathrm{MAE}(\%) = \frac{100}{N} \times \sum_1^N \left| \frac{{}^{th}X(i)^{-X}\exp(i)}{{}^{th}X(i)} \right| \tag{13}$$

Table 1
Physical properties of different nanoparticles

	Density (kg/m^3)	Specific heat (J/kg·K)	Thermal conductivity (W/m·K^{-1})
Al_2O_3	3,600	765	40
Cu	8,933	385	401
SWCNT	2,600	425	6,000
MgO	3,580	877	54.9
SiO_2	2,200	745	1.4